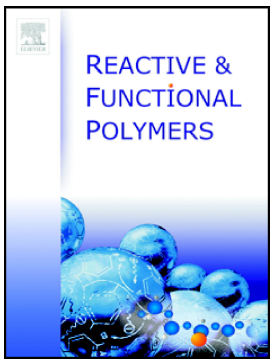

Contrastive study on β-cyclodextrin polymers resulted from different cavity-modifying molecules as efficient bi-functional adsorbents

Qi Kun Wei, Lan Bai, Xiao Mei Qin, Chunyan Hu, Lei Li, Wei Jiang, Fei Song, Yu Zhong Wang

PII: S1381-5148(19)31143-5

DOI: https://doi.org/10.1016/j.reactfunctpolym.2020.104686

Reference: REACT 104686

To appear in: *Reactive and Functional Polymers*

Received date: 2 November 2019

Revised date: 17 June 2020

Accepted date: 27 June 2020

Please cite this article as: Q.K. Wei, L. Bai, X.M. Qin, et al., Contrastive study on β-cyclodextrin polymers resulted from different cavity-modifying molecules as efficient bi-functional adsorbents, *Reactive and Functional Polymers* (2019), https://doi.org/10.1016/j.reactfunctpolym.2020.104686

Contrastive study on β-cyclodextrin polymers resulted from different cavity-modifying molecules as efficient bi-functional adsorbents

QiKun Wei, Lan Bai*, XiaoMei Qin, Chunyan Hu, Lei Li, Wei Jiang, Fei Song and YuZhong Wang

The Collaborative Innovation Center for Eco-Friendly and Fire Safety Polymeric Materials,
National Engineering Laboratory of Eco-Friendly Polymeric Materials (Sichuan),
State Key Laboratory of Polymer Materials Engineering,
College of Chemistry, Sichuan University, Chengdu 610064, China

Abstract: The adsorption capacity of existing β-CD-based adsorbents is generally restrained by the limited dimension of β-CD's inherent cavity. To find an effective way to expand the inclusion/adsorption capacity of β-CD, a series of N-containing groups, amine with straight chain, imidazole with rigid five membered ring and pyridine with rigid six-membered ring, are firstly utilized to alkylate the secondary rim of β-CD through the thiol-Michael addition. The capsulation ability of the resultant β-CD derivatives are compared and the β-CD derivatives appended with aromatic imidazole or pyridine provide extremely rich host surroundings for loading Rhodamine B (RB), which is identified by the ^{1}H NMR titration and UV-Vis spectroscopy. The bi-functional adsorbents correlative to those β-CD derivatives are then synthesized by the polymerization of vinylated β-CD and the corresponding vinyl N-containing monomers, and applied to remove RB and Cd (II) from the aqueous condition. Governed by multiple factors such as porosity, surface charge and binding affinity, the imidazole modified β-

CD adsorbent revealed the best adsorption efficiency for organic dyes and metal ions, in both single- and bi-component solutions. Our work provides effective strategy and reliable basis for the design and fabrication of β-CD-based materials with high capacity and multi-functionality.

Keywords: β-cyclodextrin; cavity expansion; host-guest inclusion; adsorption; water treatment

1. Introduction

β-Cyclodextrin (β-CD) is a unique cyclic oligosaccharide consisting of seven α-linked D-glucopyranose units[1]. The hydrophobic inner cavity of β-CD can accommodate a variety of organic substrates through host-guest inclusion[2-5]. In addition, the hydroxyl groups lining the outer surface of β-CD are easy to be decorated by functional groups[6, 7]. Therefore, the combination of these two features has allowed the preparation of a number of bi-functional β-CDs which have found a wide range of practical applications from biotherapy[8, 9] to catalysis[10], especially in simultaneous removal of metal ions and organic pollutants from contaminated water[11, 12]. If β-CDs are going to serve as adsorbents, a crucial factor to be considered is their capacity. However, existing β-CD-based adsorbents still suffer from the limited dimension of β-CD's inherent cavity which seriously restrains the adsorption efficiency of organic matters.

Modification by molecules with long linear chains or aromatic rings on the rim of the cavitand (a container-shaped host molecule[13]) is known to create a larger hydrophobic "pocket" for encapsulating more organic guests[14-16]. Inspired by this concept, lately, we constructed a bi-functional adsorbent in which the aromatic imidazole molecules were attached standing on the secondary rim of β-CD to expand the capacity of the β-CD cavity for organic dyes; meanwhile,

the nitrogen atoms of the imidazole can bind heavy metal ions[17]. Besides, very few other literatures have also reported that having both the hydrophobic space of modifying group and the cavity structure of β-CD, β-CD derivatives can provide extremely rich host surroundings for loading guest molecules[18]. However, to the best of our knowledge, the role of the modifying group's structure on the inclusion property of β-CD for organic guest has not yet been discussed.

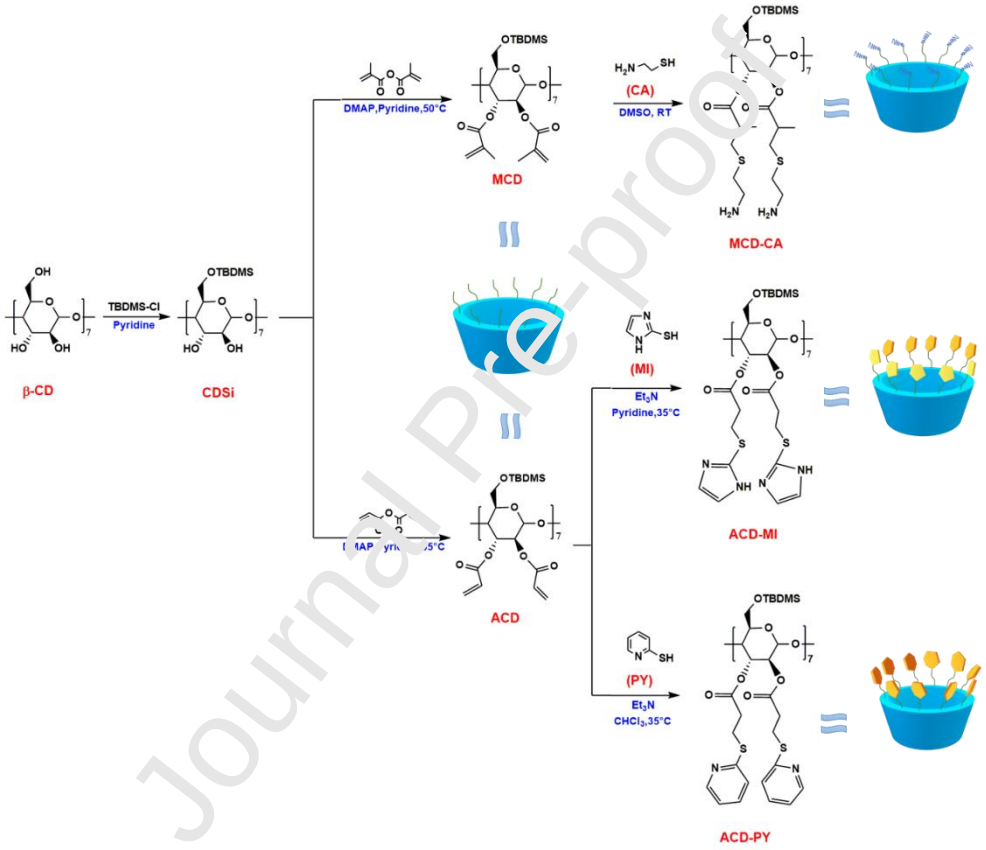

Scheme 1. Synthesis routes of β-CD derivatives.

To address the foregoing knowledge gap, in this paper, the secondary rim of β-CD was alkylated by three different N-containing groups, amine with straight chain, imidazole with rigid five-membered ring and pyridine with rigid six-membered ring, to give vase-like β-CD derivatives (Scheme 1). The inclusion properties of the β-CD derivatives were compared in

DMSO using Rhodamine B (RB), a typical dye contaminant with biological toxicity, as organic matter, considering its suitable molecular dimension and distinguishable characteristic absorption spectrum (Table S1). Then, the corresponding cavity-expanded adsorbents were obtained by the polymerization of vinylated β-CD and different vinyl monomers of amine, imidazole and pyridine, respectively (Scheme 2). Eventually, the removal of the resultant bi-functional adsorbents for RB and cadmium ion (Cd(II)) were investigated.

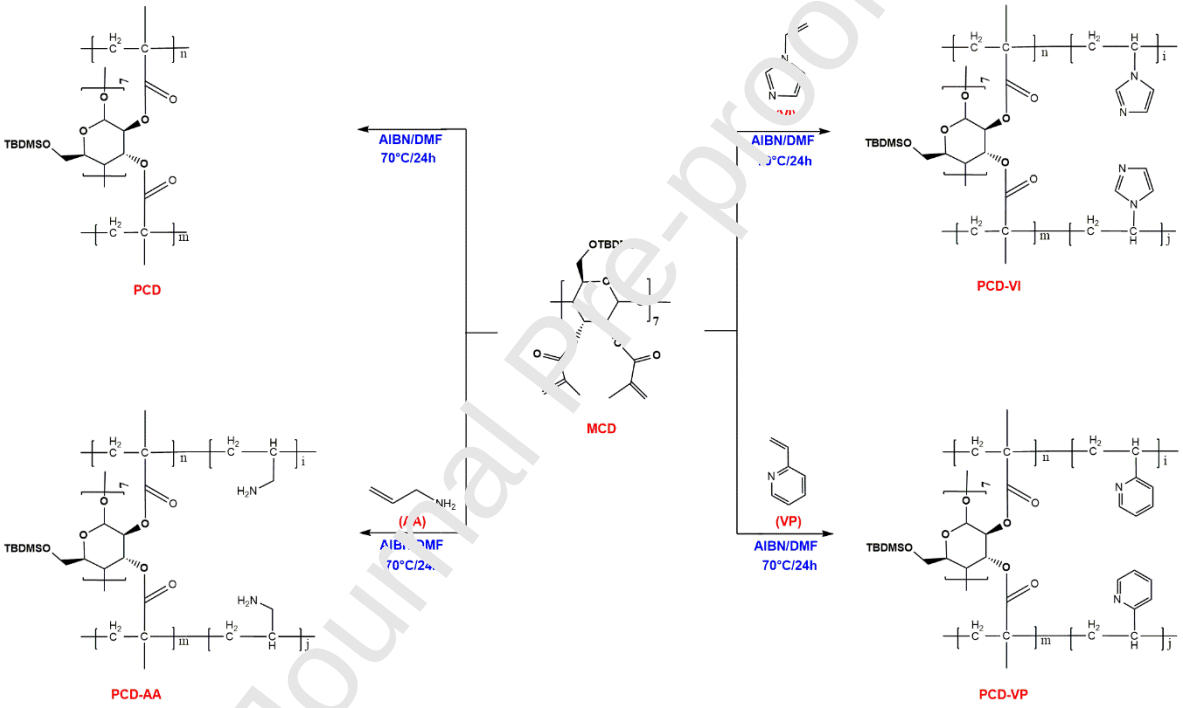

Scheme 2. Synthesis routes of polymeric absorbents.

2. Experimental Section

2.1. Materials. β-Cyclodextrin (β-CD) purchased from Aladdin Chemistry Co. Ltd. (Shanghai, China) was recrystallized three times from deionized water and dried at 70 °C for 48 h before use. tert-butylchlorodimethylsilane (TBDMS-Cl, 97%), methacrylic anhydride (MA, 94%), 4-(dimethylamino)-pyridine (DMAP, 99%), Cysteamine (CA, 95%), allylamine hydrochloride

(AA, 98%), 1-vinylimidazole (VI, 99%), 2-Vinylpyridine (VP, 97%), 2,2'-azobis (2-methylpropionitrile) (AIBN), cadmium nitrate tetrahydrate and Rhodamine B (RB) were purchased from Aladdin Chemistry Co. Ltd. (Shanghai, China). Acrylic anhydride (97%), 2-mercaptopyridine (PY, 99%) and 2-Mercaptoimidazole (MI, 98%) were purchased from Adamas Reagent CO. Ltd (Shanghai, China). Pyridine purchased from Kelong Chemical Industries Reagent Co. Ltd. (Chengdu, China) was dried over CaH_2 and distilled before use. All other chemicals were analytical grade and used without further purification. Pure water (18.2 MΩ cm at 25 °C) was obtained from a water purification system (UPH-I-20T, ULUPURE, China).

2.2. Measurements. ^{1}H NMR spectra were recorded on a Bruker Advance 400 spectrometer (Bruker, Germany) using tetramethyl silane (TMS) as an internal reference. The Ultraviolet-visible (UV-Vis) spectra were measured using a Varian Cary® 50 UV-Vis spectrophotometer (Varian Co., USA). Fourier transform infrared spectroscopy (FT-IR) was obtained on a Nicolet 6700 Fourier transform infrared spectrophotometer (Thermo Scientific Co., USA) in the 400-4000 cm^{-1} region with a resolution of 4 cm^{-1}. Elemental analysis was performed with a Euro EA 3000 elemental analyzer (Leeman Labs Inc., USA). Scanning electron microscopy (SEM) was used to characterize the sample morphology using a JSM-5900LV scanning electron microscope (JEOL Co., Japan), samples were coated with Au before the measurement. Nitrogen adsorption/desorption isotherms were obtained using a ASAP 2460 surface area analyzer (Micromeritics Co., USA), and the Brunauer-Emmett-Teller (BET) and Barret-Joyner-Halenda (BJH) methods were employed for the calculation of the specific surface area and pore size distribution, respectively. Samples were outgassed at 80 °C for 24 h before the measurement. Thermogravimetric analysis (TG) was carried out on a thermogravimetric analyzer 209 F1 (NETZSCH, Germany). The samples were heated from 40 to 700 °C at a heating rate of 10 °C

min^{-1} and the N_2 flow of 50 mL min^{-1}. The ζ-potentials of adsorbents were measured using a Zetasizer Nano ZS90 particle sizer and Zeta potential analyzer (Malvern Instruments, Ltd., UK.), with the initial solution pH ranged from 2.0 to 10.0.

2.3. Synthesis of β-CD derivatives

2.3.1. Synthesis of per-6-(tert-butyldimethylsilyl)-β-CD (CDSi). CDSi was synthesized according to the literature as follows[19]: dry β-CD (4.5 g, 4 mmol) was dissolved under vigorous stirring in anhydrous pyridine (100 mL) cooled in an ice bath. A solution of TBDMS-Cl (7.2 g, 48 mmol) in dry pyridine (40 mL) was then added dropwise to the cooled reaction vessel over 40 min. The reaction mixture was stirred for 18 h under argon atmosphere at room temperature, then the solvent was removed under reduced pressure left a white solid, which was taken up in $CHCl_3$ (100 mL). The $CHCl_3$ layer was washed by $KHSO_4$ solution (100 mL, 1 M) to remove residual pyridine, followed by saturated aqueous NaCl solution (100 mL). The organic phase was recovered and evaporated to dryness. CDSi **(**7.38 g, 96%) was recovered. ^{1}H NMR ($CDCl_3$, 400MHz): δ ppm: 0.03 (s, 21H, CH_3-Si), 0.04 (s, 21H, CH_3-Si), 0.87 (s, 63H, $(CH_3)_3C$), 3.57 (d, 7H, C(6)H of β-CD), 3.64 (m, 14H, C(2)H, C(5)H of β-CD), 3.71 (d, 7H,C(3)H of β-CD), 3.90 (d, 7H, C(6)H of β-CD), 4.02 (d, 7H, C(4)H of β-CD), 4.89 (d, 7H, C(1)H of β-CD). The molar mass of CDSi (M_{CDSi}) was calculated to be 1932 g mol^{-1}.

2.3.2. Synthesis of (2, 3-Di-O-methacrylated-6-tert-butyldimethylsilyl)-β-cyclodextrin (MCD). According to the literature[20, 21], CDSi (1.36 g), methacrylic anhydride (3.8 mL) and DMAP (0.08 g) were dissolved in pyridine (14 mL) and stirred at 50 °C overnight under nitrogen. The product was precipitated into cold water (5 °C, 120 mL), purified by reprecipitation with methanol and water, collected, and dried under vacuum. Yield: 69%. ^{1}H NMR ($CDCl_3$, 400

MHz): δ ppm: 0.04 (d, 42H, $(CH_3)_2$-Si), 0.88 (s, 63H, $(CH_3)_3C$), 1.70-2.05 (m, 30.2H, CH_3 in methacryloyl), 3.55-4.30 (m, 35H, C(3)H, C(4)H, C(5)H and C(6)H of β-CD), 4.77 (d, 7H, C(2)H of β-CD), 5.22 (s, 7H, C(1)H of β-CD), 5.62 (m, 10.9H, CH_2=C of methacryloyl), 6.11 (m, 10H, CH_2=C of methacryloyl). The molar mass of MCD (M_{MCD}) was calculated to be 2612 g mol^{-1}.

2.3.3. Synthesis of (2,3-Di-O-acrylated-6-tert-butyldimethylsilyl)-β-cyclodextrin (ACD). CDSi (1.36 g), acrylic anhydride (2.8 mL) and DMAP (0.08 g) were dissolved in pyridine (14 mL) and stirred at 35 °C overnight under nitrogen. The reacted solution was dropped into cold water, precipitated, centrifuged, washed, and dried under vacuum. ACD was obtained as brown solid. Yield: 64%. ^{1}H NMR (DMSO, 400 MHz): δ ppm: 0.05 (d, 42H, $(CH_3)_2$-Si), 0.85 (s, 63H, $(CH_3)_3C$), 3.10-4.04 (m, 35H, C(3)H, C(4)H, C(5)H and C(6)H of β-CD), 4.95-5.71 (m, 14H, C(1)H, C(2)H of β-CD), 6.11 (m, 30H, CH_2=C of acryloyl). The molar mass of ACD (M_{ACD}) was calculated to be 2472 g mol^{-1}.

2.3.4. Synthesis of cysteamine substituted β-CD derivative (MCD-CA). According to the literature[22], MCD (0.5 g) and CA (0.22 g) were dissolved in DMSO (4 mL), stirred for 12 h at room temperature. The solution was poured into CH_2Cl_2 (20 mL) and washed by saturated aqueous NaCl solution (20 mL × 3). The organic layer was evaporated to dryness to afford a brown solid with a yield of 84%.

2.3.5. Synthesis of 2-mercaptoimidazole substituted β-CD derivative (ACD-MI). ACD (0.2 g), MI (0.5 g) and Et_3N (0.10 g) were dissolved in pyridine (5 mL) and stirred for 48 h at 35 °C. The product was evaporated to dryness, the resultant residue was dissolved in $CHCl_3$ (20 mL) and

washed with saturated aqueous NaCl solution (20 mL × 3). The organic layer was then evaporated to dryness to afford a brown solid with a yield of 62%.

2.3.6. Synthesis of 2-mercaptopyridine substituted β-CD derivative (ACD-PY). ACD (0.2 g), PY (0.26 g) and Et_3N (0.05 g) were dissolved in $CHCl_3$ (6 mL) and stirred for 24 h at 35 ℃. The solution was poured into $CHCl_3$ (20 mL) and washed by saturated aqueous NaCl solution (20 mL × 3). The organic layer was evaporated to dryness to afford a brown solid with a yield of 73%.

2.4. Characterization of inclusion complexes

2.4.1. ^1H NMR titration experiments. Host/RB complexes were first prepared by a simple co-evaporation method[23]. The host and RB were dissolved in CH_2Cl_2 at a certain molar ratio (see the corresponding Fig. S7. for details), stirred at room temperature for 3 hours, and then the sample was evaporated under reduced pressure in a rotary evaporator at 40 ℃ to produce a solid inclusion complex. The ^1H NMR spectra of the hosts, RB and the inclusion complexes were then tested using deuterated DMSO-$_{d6}$ as solvent. The concentration of RB was maintained constant throughout the titration.

2.4.2. UV-Vis. The mixed solutions of RB (1.75×10^{-5} mol L^{-1}) and β-CD derivative (0.25×10^{-5} mol L^{-1}) were prepared using CH_2Cl_2 as solvent. After shaking for 3 h, the absorbance of the mixed solutions was measured by UV-Vis. The absorbance of the single solution of RB (1.75×10^{-5} mol L^{-1}) and β-CD derivatives (0.25×10^{-5} mol L^{-1}) were also determined.

2.4.3. Job's plot experiment. According to the literature[24], a set of solutions for host-guest complex were prepared varying the mole fraction of the host in the range of 0-100%. In these solutions, the total molar concentration of host and RB was fixed at 2×10^{-5} mol L^{-1}. The intensity of the UV-Vis absorption peak at 554 nm was recorded every time when changing the molar

ratio of host. The difference in absorbance of RB at 554 nm without and with hosts was calculated as ΔA, and the stoichiometry for each complex was determined by plotting ΔA against the mole fraction of the host. All the experiments were performed in CH_2Cl_2 solution.

2.5. Synthesis of the polymeric absorbents

2.5.1. Synthesis of PCD. The homopolymer of MCD (labeled PCD) was synthesized as follows: MCD (1.44 g), AIBN (0.10 g) and DMF (12 mL) were added into a round-bottomed flask and stirred for 24 h under nitrogen atmosphere at 70 °C. The PCD was precipitated from the reacted mixture by ethyl acetate, then washed with water and dried under vacuum at 40 °C.

2.5.2. Synthesis of PCD-AA. PCD-AA was synthesized from the copolymerization of MCD and AA with a molar ratio of 1:10. It was synthesized as follows: MCD (1.44 g), AA (0.52 g), AIBN (0.10 g) and DMF (14 mL) were added into a round-bottomed flask and stirred for 24 h under nitrogen atmosphere at 70 °C. The PCD-AA was precipitated from reacted mixture by ethyl acetate, stirred by water-triethylamine mixture to removal HCl, washed by water and dried under vacuum at 40 °C[25].

2.5.3. Synthesis of PCD-VI. PCD-VI was synthesized from the copolymerization of MCD and VI with a molar ratio of 1:10. It was synthesized as follows: MCD (1.44 g), VI (0.50 mL), AIBN (0.10 g) and DMF (16 mL) were added into a round-bottomed flask and stirred for 24 h under nitrogen atmosphere at 70 °C. The PCD-VI was precipitated from the reacted mixture by ethyl acetate, then washed with water and dried under vacuum at 40 °C.

2.5.4. Synthesis of PCD-VP. PCD-VP was synthesized from the copolymerization of MCD and VP with a molar ratio of 1:10. It was synthesized as follows: MCD (1.00 g), VP (0.4 mL), AIBN (0.06 g) and DMF (6 mL) were added into a round-bottomed flask and stirred for 24 h under

nitrogen atmosphere at 70 °C. The PCD-VP was precipitated from the reacted mixture by ethyl acetate, then washed with water and dried under vacuum at 40 °C.

2.6. Adsorption performance of the adsorbents. The stock aqueous solutions containing dye (RB) or metal ion (Cd(II)) were prepared, respectively. All adsorption experiments were carried out by putting 50 mL of pollutant solution into 100-mL conical flasks which were filled with 0.05 g of adsorbents in a shaking water bath at 120 rpm for 24 h (25 ± 1 °C). Adjustment of solution pH was undertaken using 0.1 mol L^{-1} NaOH or HNO_3 solution for metal ions, and 0.1 mol L^{-1} NaOH or HCl solutions for dyes, respectively. After adsorption, the adsorbents were separated by syringe filter (0.45 um pore size). The residual concentration of RB was measured by UV-Vis spectroscopy at the maximum absorbance of RB (λ_{max}: 554 nm for RB). After dilution with 2% HNO_3 solution, the metal concentrations were analyzed by an inductively coupled plasma optical atomic emission spectrometry (ICP-OES) instrument (ARCOS, SPECTRO, Germany). All the tests were conducted in triplicate, and the amounts of adsorbed pollutants were calculated according to Equation S1:

$$q_t = \frac{(C_0 - C_t) \times V}{m} \qquad \textbf{(Equation 1)}$$

where q_t (mg g^{-1}) is the amount of adsorbate adsorbed per gram of adsorbent at time t (h). C_0 (mg L^{-1}) and C_t (mg L^{-1}) are the initial and residual concentrations of adsorbate in the initial solution and filtrate, respectively. m (g) and V (L) represent the weight of the adsorbent and the volume of the solution, respectively.

2.6.1. Effect of solution pH. The effect of pH was investigated by mixing 50 mg adsorbents with 50 mL of RB (200 mg L^{-1}) or 50 mL of Cd(II) (200 mg L^{-1}) at different initial pH values under shaking for 24 h (25 ± 1 °C).

2.6.2. Adsorption isotherms. The effect of pollutant concentration on adsorption was carried out using batch experiment by putting 50 mL of adsorbate solution into a 100-mL conical flask which was filled with 50 mg of adsorbents under shaking for 24 h (25 ± 1 °C). The initial concentrations ranged from 50 to 800 mg L^{-1} both for RB and Cd(II). The initial pH values of RB and Cd(II) were adjusted to 4.0 and 6.0, respectively.

2.6.3. Simultaneous adsorption of RB and Cd(II). The experiments were conducted by mixing 50 mg adsorbents with 50 mL adsorbate solutions containing both RB and Cd(II) at pH 6 under stirring for 24 h (25 ± 1 °C). The initial concentrations of both RB and Cd(II) ranged from 50 to 300 mg/L. The results of mono-component system were utilized as references.

3. Results and Discussion

3.1. Synthesis and characterization of β-CD derivatives. To obtain a β-CD derivative in which only the secondary rim was functionalized by N-containing groups, all the seven primary hydroxy groups in the first rim of β-CD were firstly protected by TBDMS moieties, which was confirmed by the ^{1}H NMR spectrum of CDSi (Fig. S1). Then the CDSi was further reacted with methacrylic anhydride or acrylic anhydride to produce vinylated β-CD precursors MCD or ACD, in which 10/14 secondary hydroxy groups of β-CD were substituted by alkenyl groups according to the ^{1}H NMR results (Fig. S2 and S3). Due to the steric hindrance of methyl group, methacrylate modified MCD was unreactive to molecules aromatic groups during thiol-Michael

addition, which had been proved by both literature[26] and our experiments. Thus, MCD-AC, the β-CD derivative appended with linear amine, was synthesized by the reaction between cysteamine (CA) and MCD[22, 27] but the ones appended with high sterically hindered imidazole and pyridine (named as ACD-MI and ACD-PY, respectively) were obtained from methyl-free ACD[28, 29]. For all the three derivatives, the number of introduced N-containing groups in per derivative molecule was determined to be 10 according to the ^{1}H NMR results (Fig. S4~S6), which brought great convenience in comparing the influence of modifying group's structure on the inclusion performance regardless the amount of modifying group.

In addition, the chemical structures of the β-CD derivatives were characterized by FT-IR (Fig. S7). The adsorption peak at 1464 cm^{-1} of MCD was assigned to the C-H bending vibration of on -CH_3 of methacrylate group. The sharp adsorption peaks at 1729 cm^{-1} of ACD and MCD were assigned to the strong C=O stretching vibration of the methacrylate group, whereas the same peaks in MCD-AA, ACD-MI and ACD-VP appeared at 1742, 1741 and 1743cm^{-1}, respectively. In regard to MCD-AA, the signal at 1653 cm^{-1} corresponded to the bending vibration of N-H. The structure of ACD-MI was confirmed by the signals at 1259 and 1647 cm^{-1} which were atributed to the stretching vibirations of C-N and C=N in imiazole, respectively. ACD-PY revealed characteristic signal at 1578 cm^{-1}, corresponding to the stretching vibiration of C=C and C=N in pyridine ring.

3.2. Inclusion of RB by different β-CD-based hosts. Using MCD and the above three β-CD derivatives as hosts, their inclusion complexes with guest RB were denoted MCD/RB, MCD-CA/RB, ACD-MI/RB and ACD-PY/RB, respectively. The host-guest complexations were monitored in DMSO by ^{1}H NMR titration. The full ^{1}H NMR spectra of the hosts, RB and the complexes are recorded in Fig. S8 and the incepted parts are shown as Fig. 1a~d. Here, the

inclusion of RB by ACD-PY is described in detail as a representative. As shown in Fig. 1d, the addition of ACD-PY resulted in the transition of xanthene protons resonance ($H_{e,f,g}$) （Fig. S9） from broad multiplet for neat RB to sharp singlet for the complexes, attributing to the shielding effect of the electron-rich cavity of β-CD on RB[30]. In addition, the resonance signals of benzoic protons (H_a, $H_{b,c}$, H_d) and $H_{e,f,g}$ of RB experienced an upfield shift with increasing amounts of the ACD-PY, which also resulted from the shielding effect of β-CD cavity[31, 32]. However, the C-H resonances of the alkyl chain (H_h, H_i) for RB were almost unchanged before and after complexation. These phenomena indicated that the benzoic acid and xanthene groups of RB were bound within the cavity of ACD-PY, while the alkyl chains were directed toward the external space[31, 33]. Notably, the maximum upfield-change in chemical shift (Δδ) of $H_{e,f,g}$ peak was obtained in complex(1:0.33) (tagged by ▬), indicating the formation of a 1:3 (host-guest) inclusion complex[34]. From the Δδ values of $H_{e,f,g}$ peaks for all the host-RB complexes (Table S2), similarly, the maximum inclusion stoichiometries of host : RB could be determined to be 1:0.6, 1:0.6 and 1:2 for MCD/RB, MCD-CA/RB and ACD-MI/RB, respectively. Therefore, the proposed binding modes of RB by different hosts are illustrated in Fig. 1e.

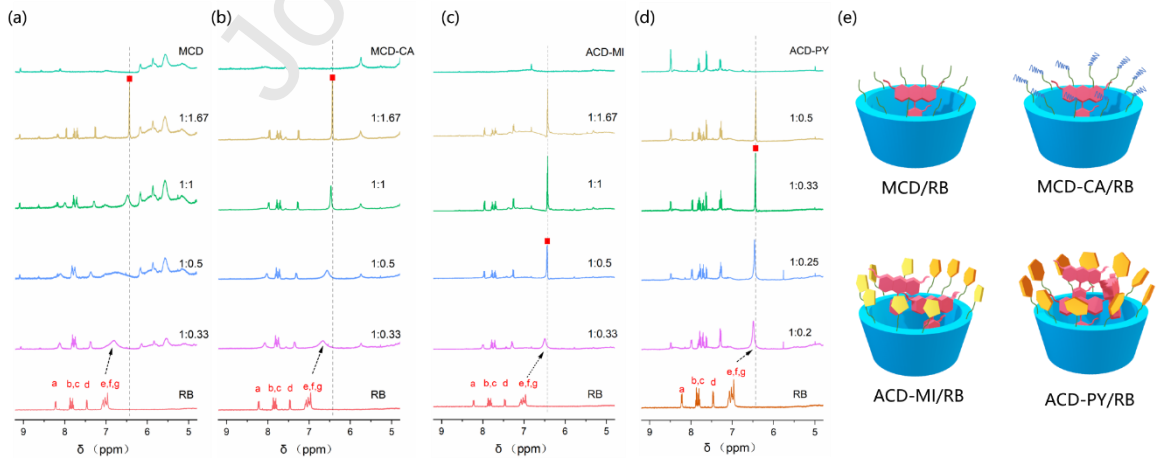

Fig. 1. ^{1}H NMR titration spectra of RB with (a)MCD, (b)MCD-CA, (c)ACD-MI and (d)ACD-PY (The molar ratios of guest: host are labeled on individual spectrum); (e) Proposed binding modes of RB by different hosts.

Complementary information of complexation was further obtained from the UV-Vis spectroscopy (Fig. 2). RB and its complexes presented the maximum absorbance at 554 nm, while the four hosts had no UV-Vis absorption in the scanned range. Once the RB was included by the hosts with different structures, its chemical environment would be different.[35] Therefore, varying reduced degrees of absorbance at 554 nm were observed for the complexes compared to neat RB, following the trend of ACD-PY/RB > ACD-MI/RB ≈ MCD-CA > MCD/RB. The stoichiometry of the inclusion complex was also explored by means of Job's method[36]. As shown in Fig. S10, the maxima of ΔA were observed at the molar fraction of 62.50%, 31.25%, 31.25% and 25% for MCD, MCD-CA, ACD-MI and ACD-PY, respectively, indicating the 1:0.6, 1:2.2, 1:2.2 and 1:3 host-guest inclusion complex stoichiometries. Although the stoichiometry data quantitatively confirmed by the Job's method differed from that of NMR titration, taken together, there was an increase in the inclusion capacity as the dimension of modifying group increased as follows: ACD-PY > ACD-MI > MCD-CA > MCD. To be specific, the rigid aromatic ring modified derivatives displayed greater molecular encapsulating capacity relative to that of the linear group modified or unmodified hosts.

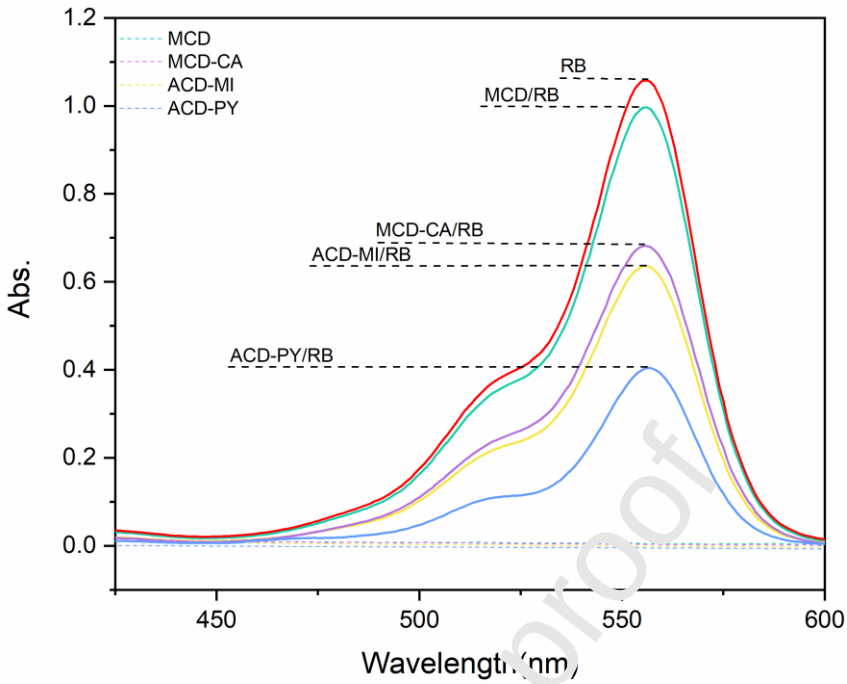

Fig. 2. UV-Vis spectra of RB, β-CD derivatives and inclusion complexes.

3.3. Synthesis and characterization of β-CD-based polymric adsorbents. To further confirm the "cavity expansion effect" of modifying groups on the β-CD's organic matter loading performance, the polymeric β-CD-based adsorbents correlative to those β-CD derivatives were synthesized by the polymerization of vinylated β-CD (MCD) and the vinyl monomers of amine, imidazole and pyridine. The resultant adsorbents were labeled PCD-AA, PCD-VI and PCD-VP, respectively (Scheme 2)

The chemical structures of PCD-AA, PCD-VI, PCD-VP, as well as PCD (a homopolymer of MCD), were confirmed by FT-IR. As shown in Fig. 3a, PCD showed the strong C=O stretching vibration (1729 cm^{-1}) of the methacrylate group and the C-O stretching vibration (1036 cm^{-1}) of the β-CD's glucose ring; the broad peaks around 3500 cm^{-1} were the signals of O-H stretching vibration of unsubstituted O-H on β-CD[37]. PCD-AA was evidenced by the bending vibration of N-H (1653 cm^{-1}). In regard to PCD-VI, the C=O stretching vibration (1730 cm^{-1}) of the

methacrylate group, and the C=N (1500 cm^{-1}) and C-N (1229 cm^{-1}) stretching vibration of the imidazole ring were observed[38-40]. The structure of PCD-VP was mainly characterized by the C=C (1599 cm^{-1}) and C=N (1416 cm^{-1}) stretching vibration in pyridine[41, 42]. In addition, the molar contents of modifying groups in PCD-AA, PCD-VI and PCD-VP were calculated to be 2.154， 2.091 and 2.255 mmol g^{-1}, respectively, based on the quantitative N elemental analysis results (Table S3). Scanning electron microscopy (SEM) images indicated the rough surface of these obtained adsorbents (Fig. 3b). In addition, the BET surface area, cumulative pore volume and average pore diameter of the adsorbents were further verified by N_2 adsorption-desorption analysis (Table S4). It was evidently that among the adsorbents, PCD-VI exhibited the most significant porosity, which implied a superior pollutant uptake property. The adsorbents also possessed good stability (Fig. S11). The thermal event at approximately 100 °C was assigned to evaporative loss of adsorbed water on the adsorbent, and another around 260 ~ 440 °C was ascribed to the decomposition of organic components.

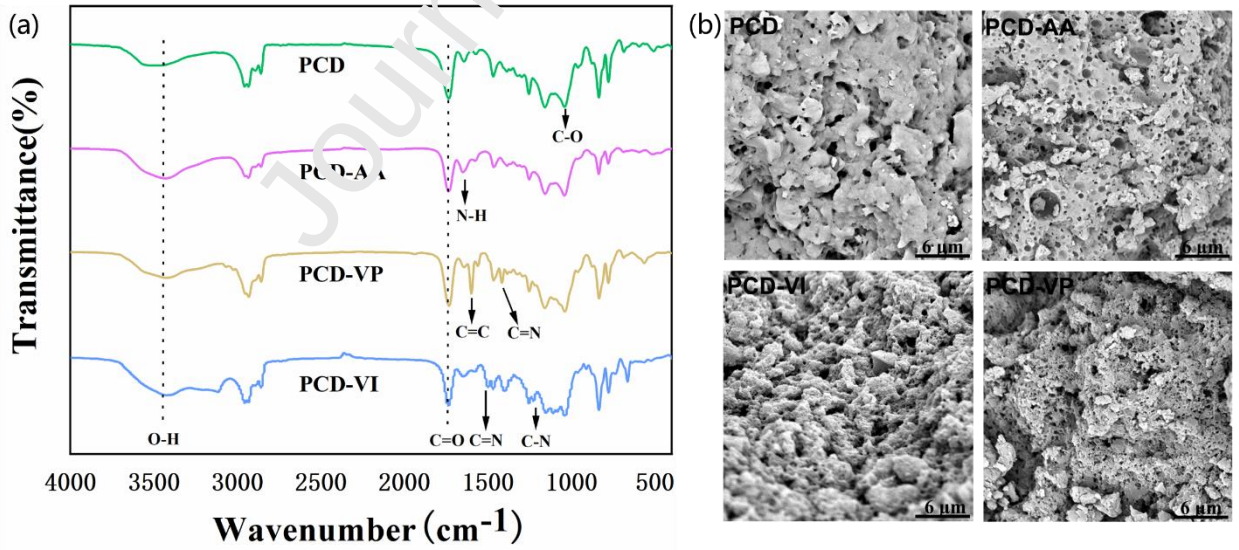

Fig. 3. (a) FTIR spectra and (b) SEM images of PCD, PCD-AA, PCD-VI and PCD-VP.

3.4. Adsorption performance of polymeric absorbents. As promising candidates for simultaneous removal of organic dyes and heavy metal ions, the adsorption characteristics of these adsorbents toward RB and Cd(II) were investigated in detail. The pH of solution is known to affect the surface charge and the ionization degree of both adsorbent and adsorbate, therefore, the adsorption performance of the four adsorbents under varied pH condition were tested. As depicted in Fig. 4a, the adsorption amounts of PCD toward RB were rather low and changed little in the experimental pH range, which mainly due to its low specific surface area, weak porosity, especially the limited capacity of β-CD's inherent cavity. PCD-AA exhibited poor adsorption capacity almost identical to PCD, suggesting the inefficient "cavity expansion" by linear amine. As to PCD-VP, although its corresponding host molecule ACD-PY possessed the highest RB inclusion amount, it only showed a slightly better adsorption capacity relative to that of PCD and PCD-AA. Its adsorption capacities increased mildly as the pH value increased, simply due to its continuously reducing positive ζ-potential (Fig. 5) which enhanced the electrostatic attraction between the pyridine groups and RB. However, altering pyridine to imidazole, the resultant PCD-VI showed the highest adsorption amount and obviously pH-dependent adsorption character. The RB adsorption by PCD-VI was little at pH 2.0, ascribing to the strong electrostatic repulsion between the protonated imidazole groups and cationic RB. With the pH value increased from 2.0 to 4.0, the adsorption of RB on PCD-VI increased dramatically, attributing to the decreased ζ-potential which facilitated the electrostatic attraction of imidazole groups to cationic RB. With the further increasing of pH from 4 to 10, the adsorption capacities remained almost consistent, that was because the changing surface charges of PCD-VI had no further electronic effect on RB adsorption in this pH range. This result suggested that the RB

adsorption was mainly dominated by the inherent cavity of β-CD and the imidazole expanded hydrophobic space, which had been confirmed by our previous study[17].

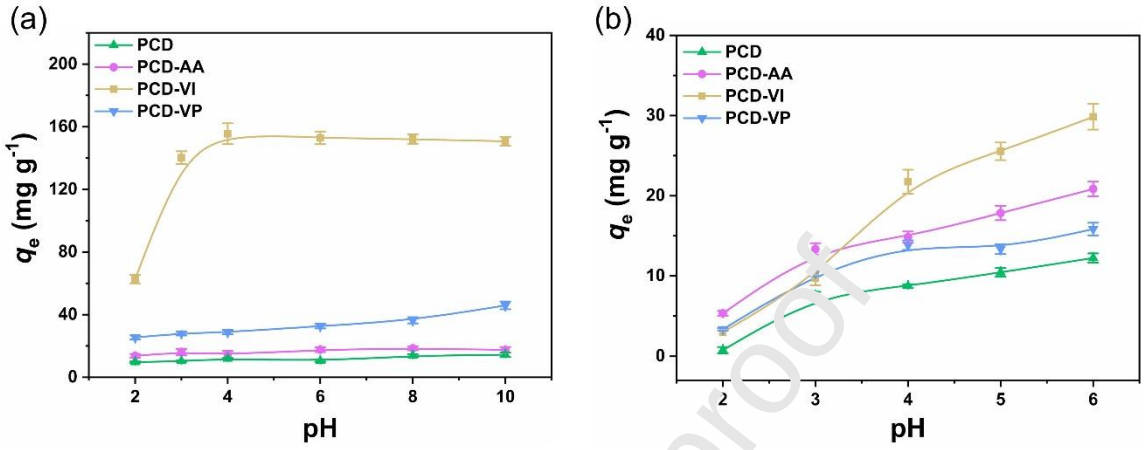

Fig. 4. The effect of pH on RB adsorption (a) and Cd(II) adsorption (b) by PCD, PCD-AA, PCD-VI and PCD-VP.

Unlike RB, the adsorption of Cd(II) by the four adsorbents all showed significantly pH-dependent characters (Fig. 4b). The reasons for the different Cd(II) adsorption capacities of the four adsorbents could be summarized into the following aspects: 1) Surface area. The surface areas of PCD, PCD-AA and PCD-VP were less than 100 m^2 g^{-1} while that of PCD-VI reached up to 300 m^2 g^{-1} (Table S4). 2) ζ-Potential. At the pH conditions herein, the values of ζ-potentials for the adsorbents followed the order of PCD-VP > PCD-VI ≈ PCD-AA > PCD. The higher ζ-potential value, the greater electrostatic repulsion between the adsorbents and metal cations. 3) Coordination affinity. Since the molar contents of the modifying groups in different adsorbents were almost identical (approximately 2 mmol g^{-1}, Table S3), the different Cd(II) coordination capacities were mainly caused by their structural differences. As evidenced by literature, among the three N-containing molecules, imidazole had the strongest coordination affinity to Zn(II),

followed by ammonia and pyridine[43]. Given that both cadmium and zinc are IIB subgroup elements, we suspected that the coordination affinity of the modifying groups to Cd(II) similarly followed the order of imidazole > amine > pyridine.

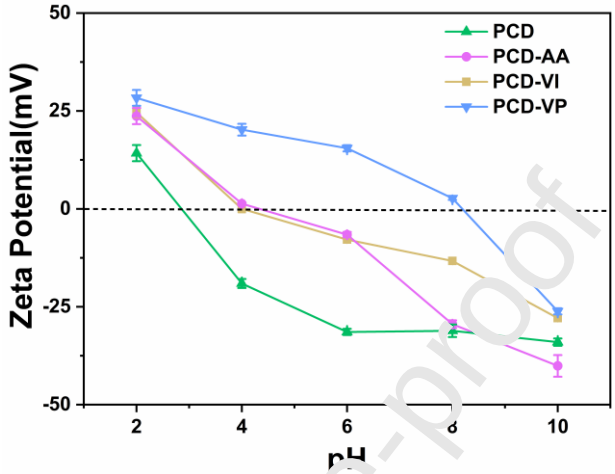

Fig. 5. Zeta potential curves of PCD, PCD-AA, PCD-VI and PCD-VP.

In general, influenced by multifarious factors, PCD-VI revealed the highest efficiency for the adsorption of both RB and Cd(II). The maximum adsorption capacities of the four adsorbents for RB and Cd(II) confirmed by isothermal adsorption, as well as the adsorption amounts of some other β-CD-based adsorbents were summarized in Table S5. Compared with those adsorbents which removed RB mainly relied on their inherent cavities, the rigid aromatic ligand modified PCD-VI exhibited superior dye adsorption capacity (Fig. S12); by virtue of the excellent metal coordination ability of imidazole, the Cd(II) adsorption capacity of PCD-VI was also acceptable (Fig. S13).

Finally, we applied the adsorbents as bi-functional materials to simultaneously remove RB and Cd(II) from RB-Cd(II) bi-component solutions. Despite of their weak capacities, PCD, PCD-AA and PCD-VP still exhibited identical adsorption efficiencies for RB and Cd(II) in the bi-

component solutions compared to that in the one-component solutions (Fig. S14). As to PCD-VI (Fig. 6), no obvious competition adsorption was observed in the adsorption of Cd(II) and the uptake of RB was even promoted in the bi-component solutions.

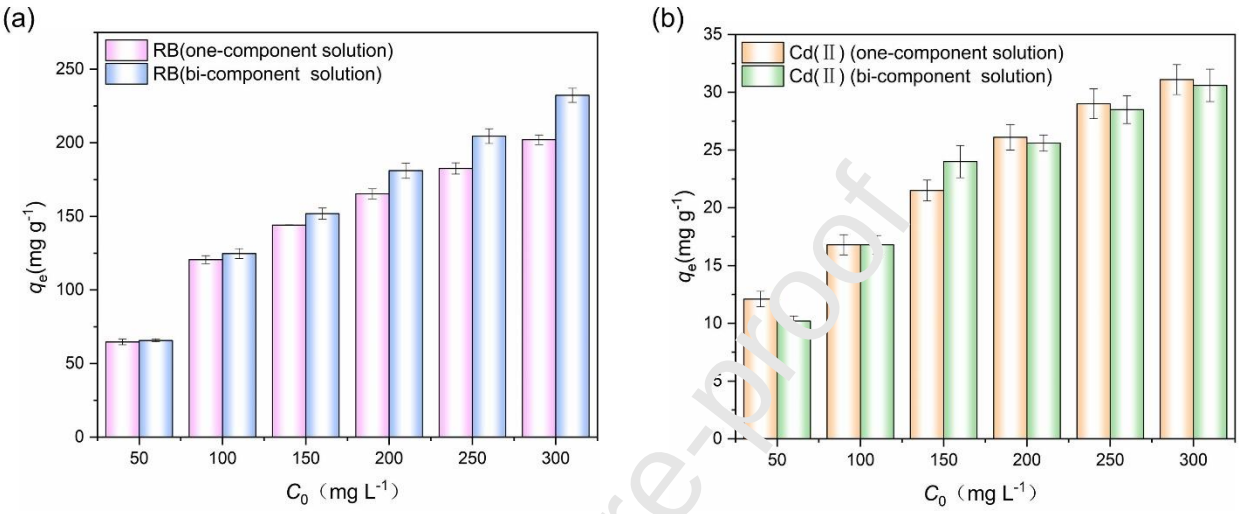

Fig. 6. Adsorption curves of RB (a) and Cd(II) (b) by PCD-VI in one-component solution and bi-component solution at pH 6.0.

Conclusions

In summary, we constructed different β-CD derivatives bearing linear or aromatic N-containing groups, made contrastive studies on their inclusion capacities as well as the adsorption properties of their corresponding polymeric adsorbents. With the help of the rigid ring expanded space, ACD-MI and ACD-PY exhibited significantly enhanced inclusion abilities toward RB as compared with MCD-CA and unmodified MCD. ACD-PY possessed the maximum cavity which can encapsulate even three guest RB molecules. However, governed by multiple factors such as porosity, surface charge and "cavity expansion effect", the imidazole modified PCD-VI revealed the best adsorption performance for RB and Cd(II) in the aqueous condition. The present results

provide an efficient strategy for expanding the limited volume of β-CD's inherent cavity and will be helpful for the design and application of β-CD-based functional molecules and materials.

Declaration of Competing Interest

The authors have declared no competing financial interest.

Acknowledgment

Financial support from the National Natural Science Foundation of China (Grant Nos. 51603129 and 51721091) is acknowledged.

Appendix A. Supplementary data

Supplementary data to this article can be found online

References

[1] G. Crini, Review: A History of Cyclodextrins, Chem. Rev., 114 (2014) 10940-10975.

[2] R. Zhao, Y. Wang, X. Li, B. Sun, C. Wang, Synthesis of β-cyclodextrin-based electrospun nanofiber membranes for highly efficient adsorption and separation of methylene blue, ACS Appl. Mater. Inter., 7 (2015) 26649-26657.

[3] W.C.E. Schofield, C.D. Dain, J.P.S. Badyal, Cyclodextrin-Functionalized Hierarchical Porous Architectures for High-Throughput Capture and Release of Organic Pollutants from Wastewater, Chem. Mater., 24 (2012) 1645-1653.

[4] A. Alsbaiee, B.J. Smith, L. Xiao, Y. Ling, D.E. Helbling, W.R. Dichtel, Rapid removal of organic micropollutants from water by a porous β-cyclodextrin polymer, Nature, 529 (2015) 190.

[5] F. Fang, X.-J. Huang, Y.-Z. Guo, X. Hong, H.-M. Wu, R. Liu, D.-J. Chen, Selective and Regenerable Surface Based on β-Cyclodextrin for Low-Density Lipoprotein Adsorption, Langmuir, 34 (2018) 8163-8169.

[6] S.-S. Zhai, Y. Chen, Y. Liu, Selective binding of bile salts by β-cyclodextrin derivatives with appended quinolyl arms, Chin. Chem. Lett., 24 (2013) 442-446.

[7] N. Vurgun, M. Nitz, Highly Functionalized β - Cyclodextrins by Solid - Supported Synthesis, Chem.-Eur. J.,

24 (2018) 4459-4467.

[8] X. Lu, Y. Ping, F. Xu, Z. Li, Q. Wang, J. Chen, W. Yang, G. Tang, Bifunctional conjugates comprising β-cyclodextrin, polyethylenimine, and 5-fluoro-2′-deoxyuridine for drug delivery and gene transfer, Bioconjug. Chem., 21 (2010) 1855-1863.

[9] V. Oliveri, F. Bellia, G. Vecchio, Cyclodextrin Nanoparticles Bearing 8‐Hydroxyquinoline Ligands as Multifunctional Biomaterials, Chem.-Eur. J., 23 (2017) 4442-4449.

[10] Y. Kang, L. Zhou, X. Li, J. Yuan, β-Cyclodextrin-modified hybrid magnetic nanoparticles for catalysis and adsorption, J. Mater. Chem., 21 (2011) 3704-3710.

[11] A.Z.M. Badruddoza, B. Bhattarai, R.P. Suri, Environmentally Friendly β-Cyclodextrin–Ionic Liquid Polyurethane-Modified Magnetic Sorbent for the Removal of PFOA, PFOS, and Cr (VI) from Water, ACS Sustainable Chem. Eng., 5 (2017) 9223-9232.

[12] F. Zhao, E. Repo, D. Yin, Y. Meng, S. Jafari, M. Sillanpää, EDTA-cross-linked β-cyclodextrin: an environmentally friendly bifunctional adsorbent for simultaneous adsorption of metals and cationic dyes, Environ. Sci. Technol., 49 (2015) 10570-10580.

[13] D.J. Cram, Cavitands: organic hosts with enforced cavities, Science, 219 (1983) 1177-1183.

[14] H. Xi, C.L.D. Gibb, B.C. Gibb, Functionalized Deep-Cavity Cavitands, J.org.chem, 64 (1999) 9286-9288.

[15] S.M. Biros, J. Rebek, Structure and Binding Properties of Water-Soluble Cavitands and Capsules, Chem. Soc. Rev., 38 (2007) 93-104.

[16] J. Kubitschke, S. Javor, J. Rebek, Deep cavitand vesicles–multicompartmental hosts, Chem. Commun., 48 (2012) 9251-9253.

[17] X. Qin, L. Bai, Y. Tan, L. Li, F. Song, Y. Wang, β-Cyclodextrin-crosslinked polymeric adsorbent for simultaneous removal and stepwise recovery of organic dyes and heavy metal ions: Fabrication, performance and mechanisms, Chem. Eng. J., 372 (2019) 1007-1018.

[18] Y. Liu, X.-Q. Li, Y. Chen, X.-D. Guan, Spectrophotometric study of selective binding behaviors of dye molecules by pyridine-and bipyridine-modified β-cyclodextrin derivatives with a functional tether in aqueous solution, J. Phys. Chem. B, 108 (2004) 19541-19549.

[19] P.F. Gou, W.P. Zhu, Z.Q. Shen, Synthesis, Self-Assembly, and Drug-Loading Capacity of Well-Defined Cyclodextrin-Centered Drug-Conjugated Amphiphilic A14B7 Miktoarm Star Copolymers Based on Poly(ε-

caprolactone) and Poly(ethylene glycol), Biomacromolecules, 11 (2010) 934-943.

[20] S. Shao, J. Si, J. Tang, M. Sui, Y. Shen, Jellyfish-Shaped Amphiphilic Dendrimers: Synthesis and Formation of Extremely Uniform Aggregates, Macromolecules, 47 (2014) 916-921.

[21] R.S. And, K. Yamaguchi, Synthesis of Bimodal Methacrylic Acid Oligomers by Template Polymerization, Macromolecules, 36 (2003) 9005-9013.

[22] X. Ma, J. Tang, Y. Shen, M. Fan, H. Tang, M. Radosz, Facile synthesis of polyester dendrimers from sequential click coupling of asymmetrical monomers, J. Am. Chem. Soc., 131 (2009) 14795-14803.

[23] Y. Wei, J. Zhang, Y. Zhou, W. Bei, Y. Li, Q. Yuan, H. Liang, Characterization of glabridin/hydroxypropyl-β-cyclodextrin inclusion complex with robust solubility and enhanced bioactivity, Carbohydr. Polym., 159 (2017) 152-160.

[24] J.S. Renny, L.L. Tomasevich, E.H. Tallmadge, D.B. Collum, Method of Continuous Variations: Applications of Job Plots to the Study of Molecular Associations in Organometallic Chemistry, Angew. Chem. Int. Ed., 52 (2013) 11998-12013.

[25] X.L. Guo, K.S. Yang, J.Y. Hyun, W.S. Kim, D.H. Lee, K.E. Min, L.S. Park, K.H. Seo, Y.I. Kim, C.S. Cho, Morphology and metabolism of Ba-alginate-encapsulated hepatocytes with galactosylated chitosan and poly(vinyl alcohol) as extracellular matrices, J. Biomater. Sci., Polym. Ed., 14 (2003) 551-565.

[26] D.P. Nair, M. Podgorski, S. Chatani, T. Gong, W. Xi, C.R. Fenoli, C.N. Bowman, The thiol-Michael addition click reaction: a powerful and widely used tool in materials chemistry, Chem. Mater., 26 (2013) 724-744.

[27] J. Tang, X. Wang, X. Wang, M. Sui, W. Mao, Y. Shen, β-Cyclodextrin-based biodegradable dendrimers for drug delivery, J. Control. Release, 152 (2011) 89-90.

[28] A. Nebioglu, J.A. Leon, I.V. Khudyakov, New UV-curable high refractive index oligomers, Ind. Eng. Chem. Res., 47 (2008) 2155-2159.

[29] J.D. Flores, N.J. Treat, A.W. York, C.L. McCormick, Facile, modular transformations of RAFT block copolymers via sequential isocyanate and thiol-ene reactions, Poly. Chem., 2 (2011) 1976-1985.

[30] L. Escobar, A. Díaz-Moscoso, P. Ballester, Conformational selectivity and high-affinity binding in the complexation of N-phenyl amides in water by a phenyl extended calix [4] pyrrole, Chem. Sci., 9 (2018) 7186-7192.

[31] I. Morenovilloslada, R. Gonzalez, S. Hess, B.L. Rivas, T. Shibue, H. Nishide, Complex formation between rhodamine B and poly(sodium 4-styrenesulfonate) studied by 1H-NMR, J. Phys. Chem. B, 110 (2006) 21576-21581.

[32] Y.-S. Zhang, R. Balamurugan, J.-C. Lin, S. Fitriyani, J.-H. Liu, A. Emelyanenko, Pd 2+ fluorescent sensors based on amino and imino derivatives of rhodamine and improvement of water solubility by the formation of inclusion complexes with β-cyclodextrin, Analyst, 142 (2017) 1536-1544.

[33] D. Zhang, C. Yang, Z. Niu, C. Wang, S. Mukherjee, D. Wang, X. Li, R. Liu, J. Gao, Y. Chen, Construction of Crowning β-cyclodextrin with Temperature Response and Efficient Properties of Host–Guest Inclusion, Langmuir, 34 (2018) 11567-11574.

[34] Q.-X. Guo, Z.-Z. Li, T. Ren, X.-Q. Zhu, Y.-C. Liu, Inclusion complexation of sodium alkyl sulfates withβ-cyclodextrin. A 1 H NMR study, J. Inclusion Phenom. Mol. Recognit. Chem., 17 (1994) 149-156.

[35] A. Rescifina, E. Surdo, V. Cardile, R. Avola, A.C.E. Graziano, R. Stancanelli, S. Tommasini, V. Pistarà, C.A. Ventura, Gemcitabine anticancer activity enhancement by water soluble celecoxib/sulfobutyl ether-β-cyclodextrin inclusion complex, Carbohydr. Polym., 206 (2019) 792-800.

[36] N. Qiu, X. Zhao, Q. Liu, B. Shen, J. Liu, X. Li, L. An, Inclusion complex of emodin with hydroxypropyl-β-cyclodextrin: Preparation, physicochemical and biological properties, J. Mol. Liq., (2019) 111151.

[37] Y. Zhou, Y. Hu, W. Huang, G. Cheng, C. Cui, J. Liu, A novel amphoteric β-cyclodextrin-based adsorbent for simultaneous removal of cationic/anionic dyes and bisphenol A, Chem. Eng. J., 341 (2018) 47-57.

[38] N. Pekel, O. Güven, Synthesis and characterization of poly (N‐vinyl imidazole) hydrogels crosslinked by gamma irradiation, Polym. Int., 51 (2002) 1401-1410.

[39] Y. Han, W. Li, J. Zhang, H. Meng, Y. Xu, X. Zhang, Adsorption behavior of Rhodamine B on nanoporous polymers, Rsc Advances, 5 (2015) 104915-104922.

[40] M. Erdem, Ö. Dikişler, F. Erdem, Removal of Orange II from aqueous solutions using N-vinyl imidazole-based hydrogels as adsorbents, Chem. Eng. Commun., 203 (2016) 1403-1412.

[41] B. Grzyb, J. Machnikowski, J. Weber, Mechanism of co-pyrolysis of coal-tar pitch with polyvinylpyridine, J. Anal. Appl. Pyrolysis, 72 (2004) 121-130.

[42] N.G. Khaligh, F. Shirini, Preparation, characterization and use of poly (4-vinylpyridinium) hydrogen sulfate salt as an eco-benign, efficient and reusable solid acid catalyst for the chemoselective 1, 1-diacetate protection and deprotection of aldehydes, J. Mol. Catal. A: Chem., 348 (2011) 20-29.

[43] D. Banerjea, T.A. Kaden, H. Sigel, Enhanced stability of ternary complexes in solution through the participation of heteroaromatic N bases. Comparison of the coordination tendency of pyridine, imidazole, ammonia,

acetate, and hydrogen phosphate toward metal ion nitrilotriacetate complexes, Inorg. Chem., 20 (1981) 2586-2590.

Author Statement

QiKun Wei：Conceptualization, Investigation, Writing - Original Draft

Lan Bai: Conceptualization, Writing - Review & Editing, Supervision

XiaoMei Qin: Investigation

Chunyan Hu: Investigation

Lei Li: Investigation

Wei Jiang: Investigation

Fei Song: Writing - Review & Editing

YuZhong Wang: Acquisition of the financial support for the project leading to this publication

Declaration of interests

☒ The authors declare that they have no known competing financial interests or personal relationships that could have appeared to influence the work reported in this paper.

Graphical Abstract

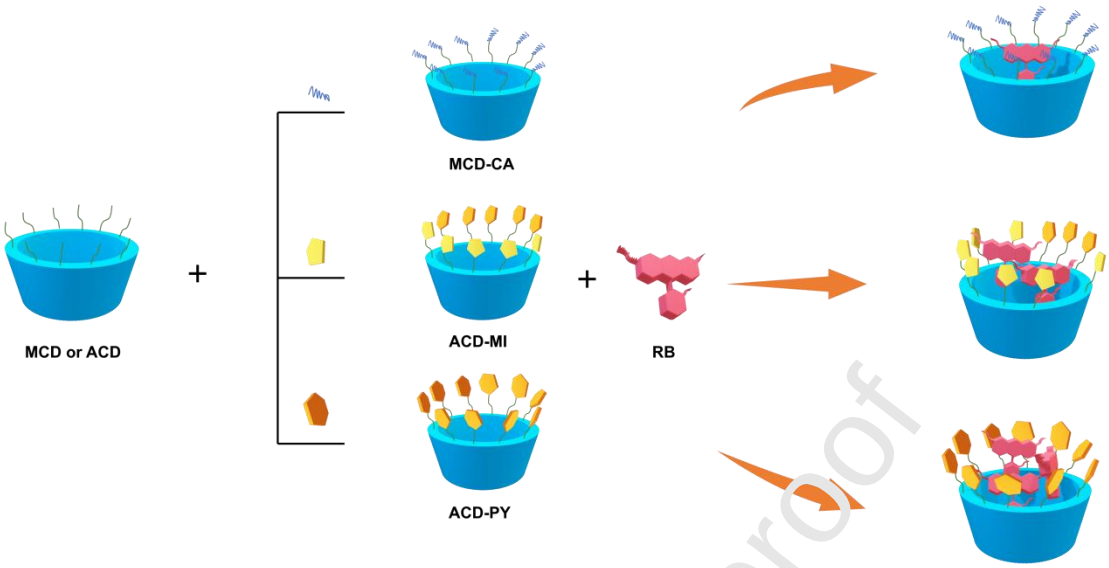

Highlights

1. A series of cavity-extended β-CD derivatives were synthesized for RB inclusion.
2. Inclusion capacities of those β-CD derivatives were characterized and compared.
3. Aromatic molecule modified β-CD derivatives provided richer host surroundings.
4. Polymeric adsorbents correlative to those β-CD derivatives were further created.
5. PCD-VI showed the optimal simultaneous removal performance of RB and Cd (II).